Table of Content:

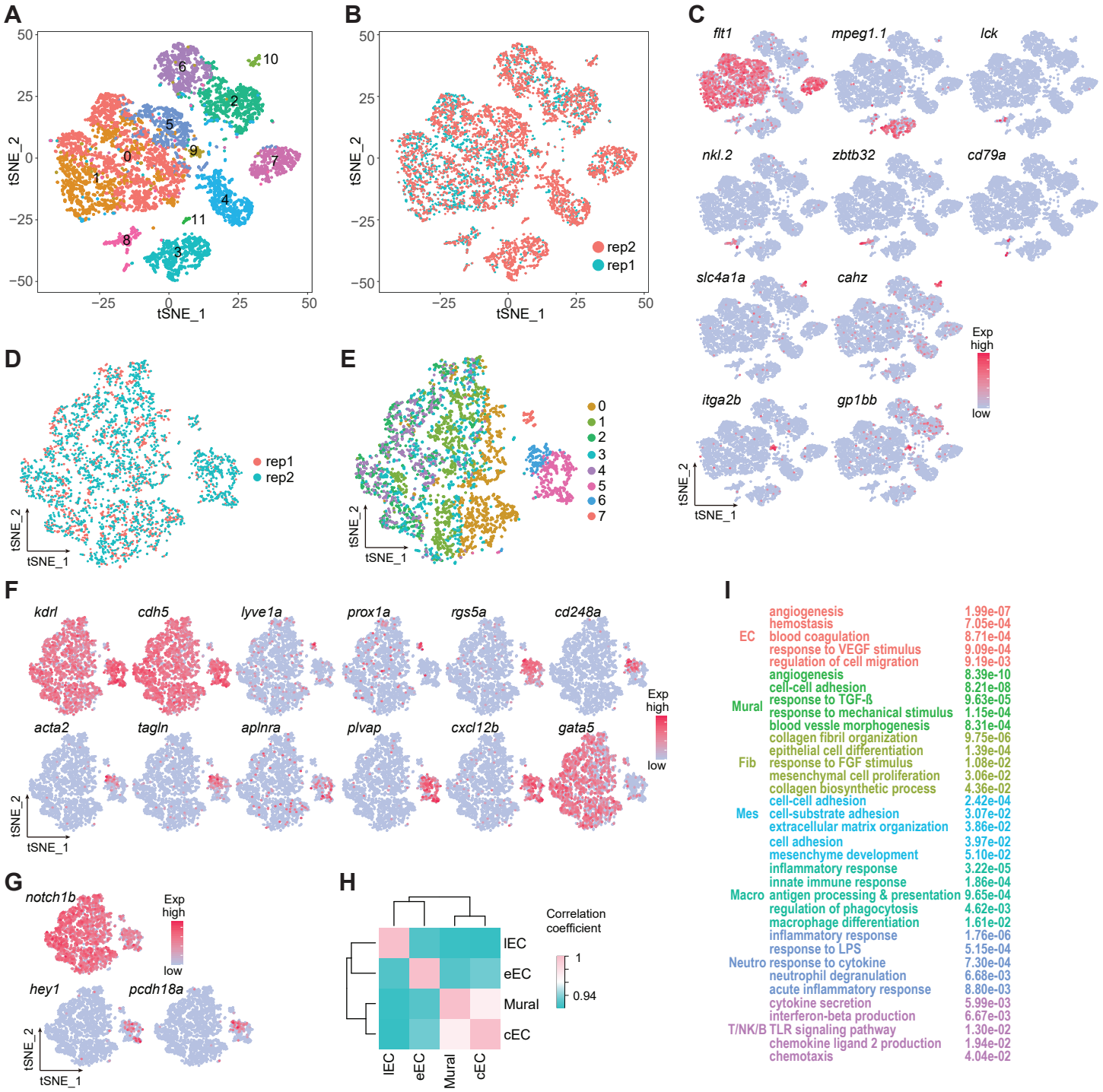

Appendix Figure S1

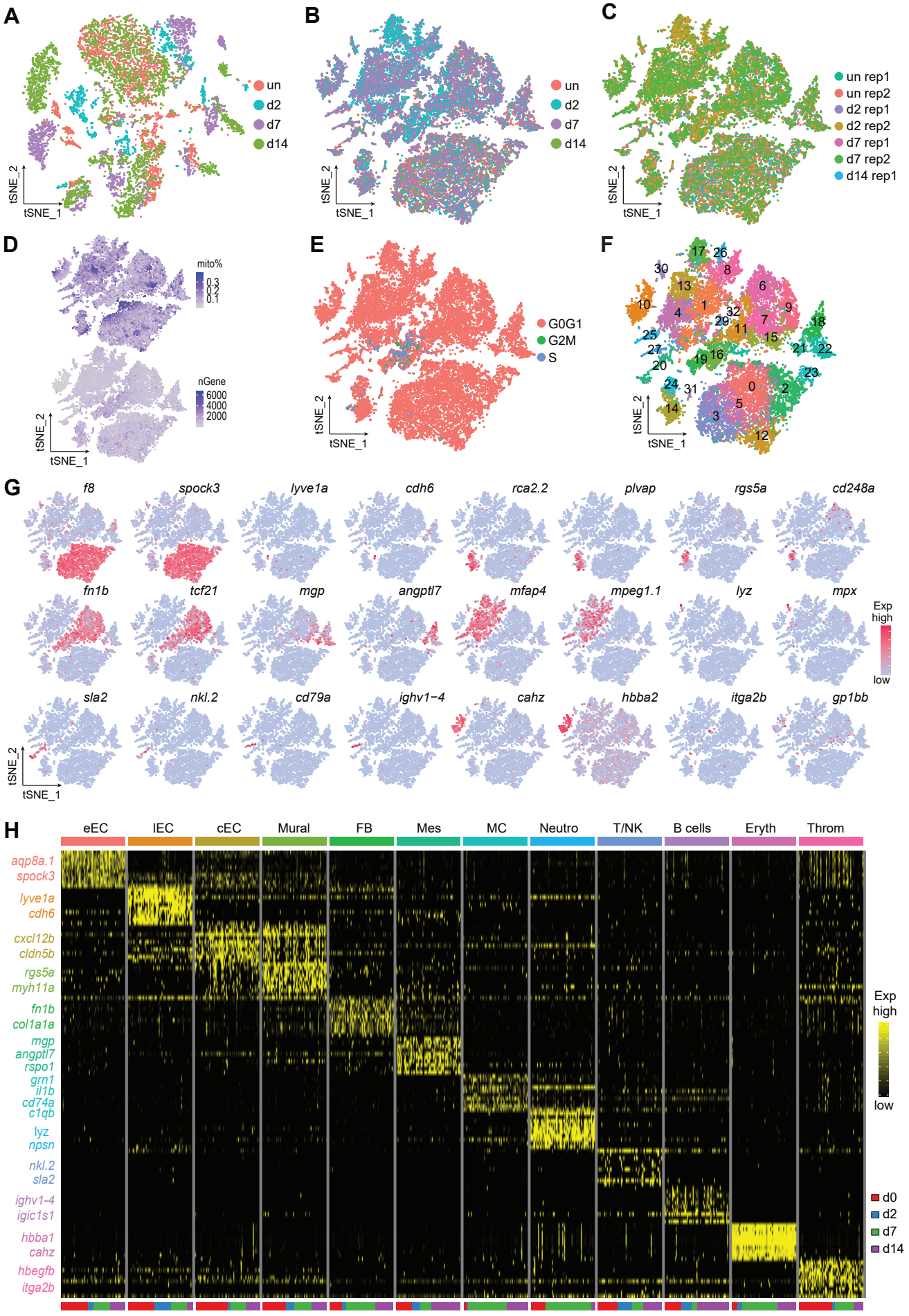

Appendix Figure S2

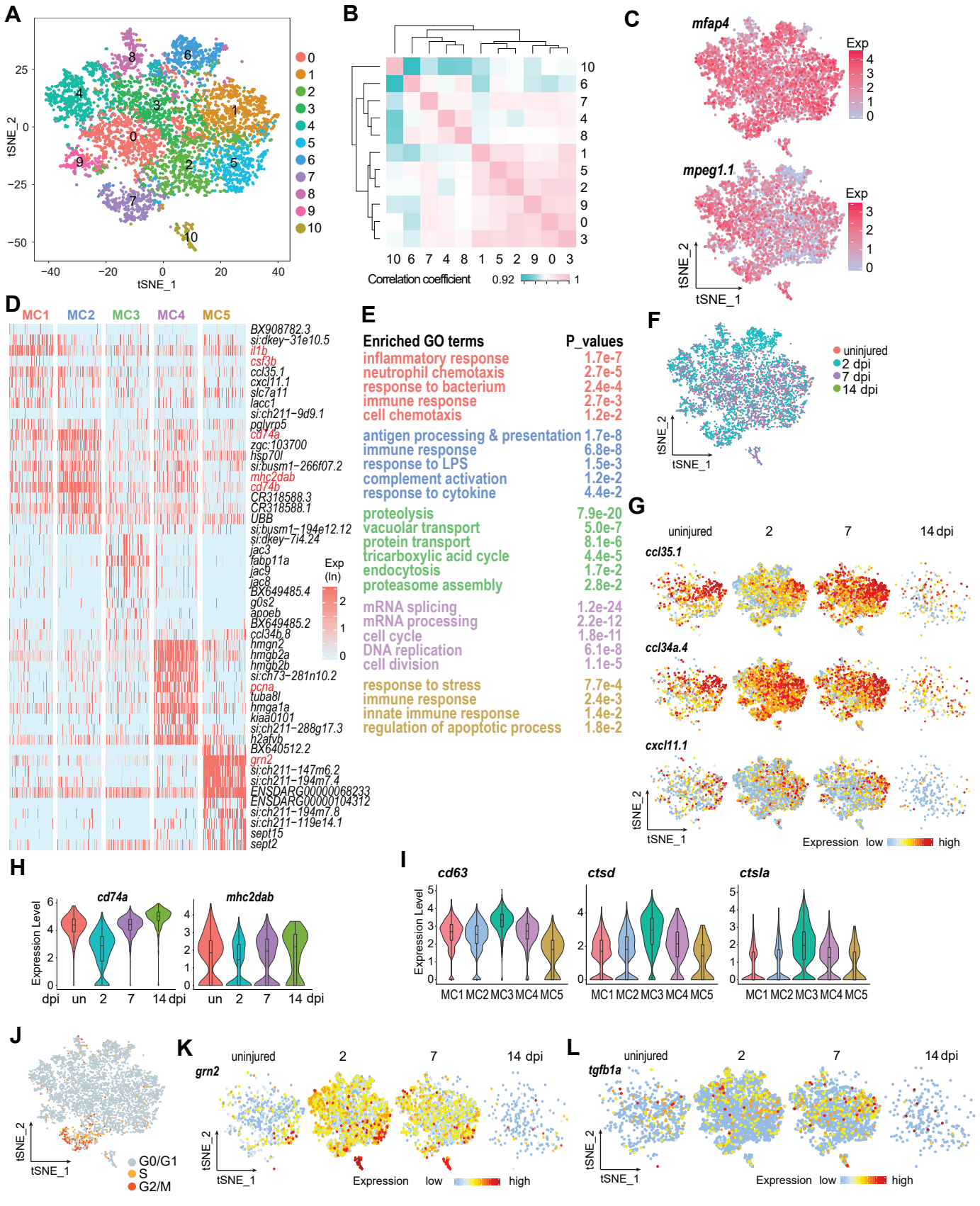

Appendix Figure S3

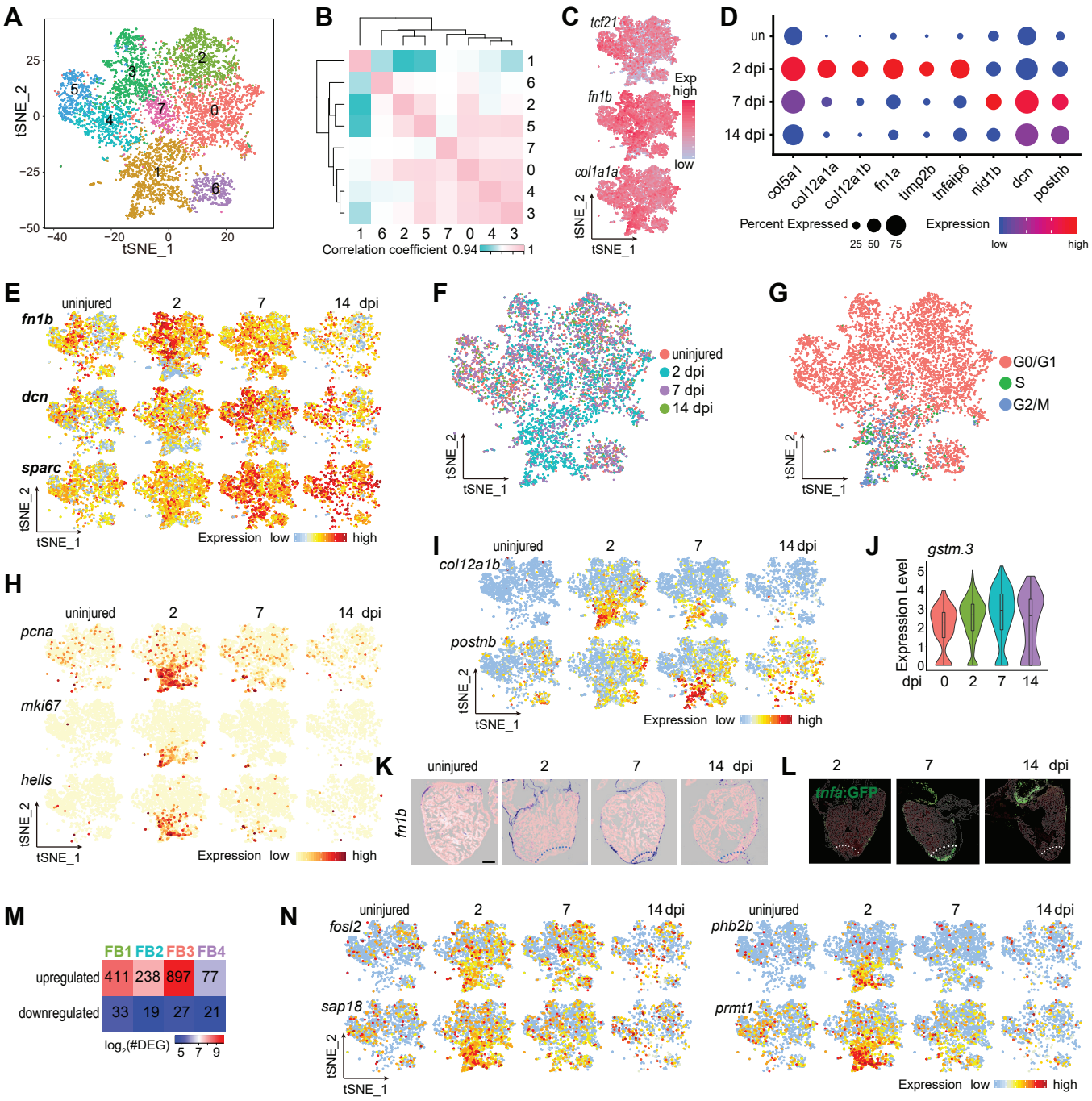

Appendix Figure S4

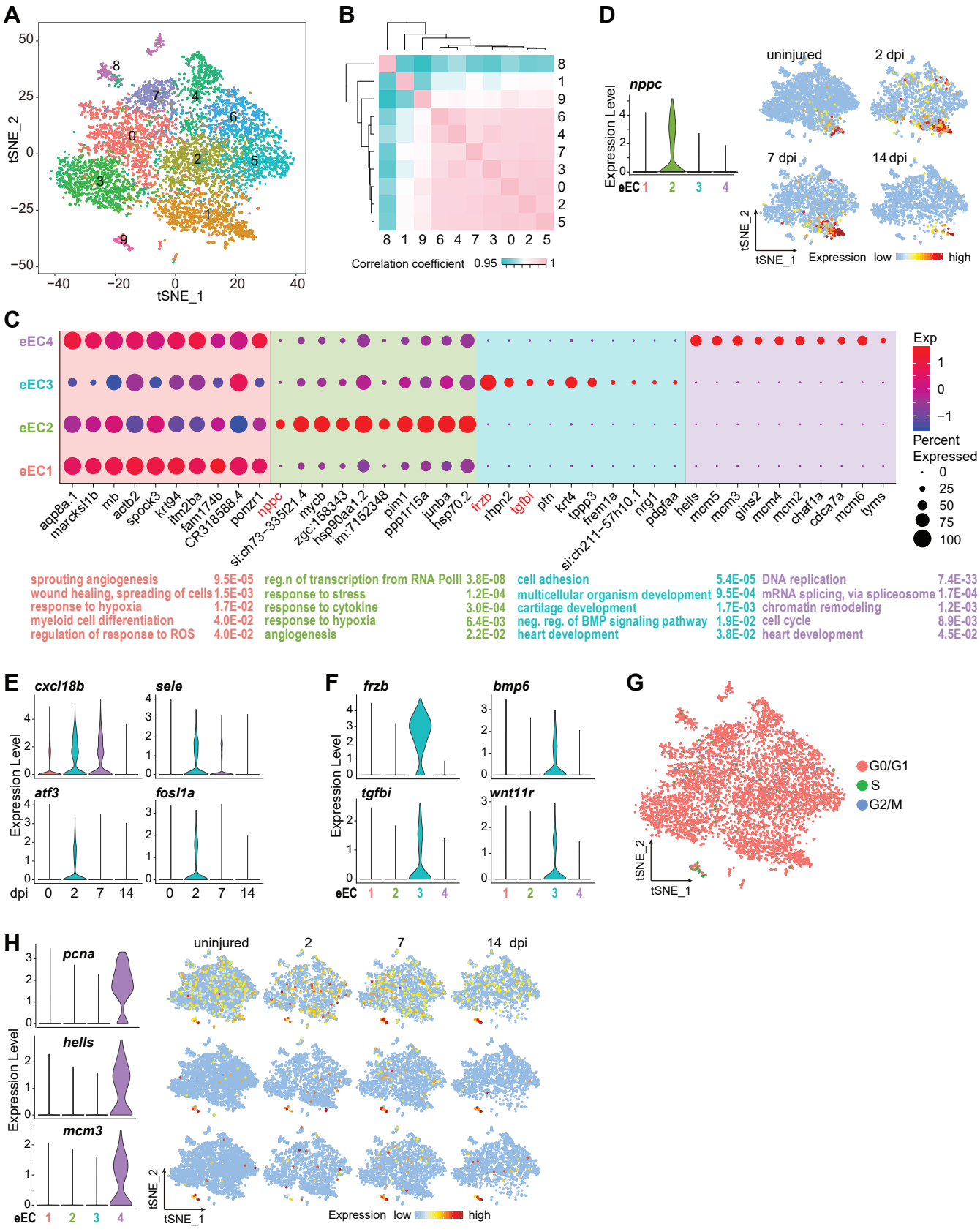

Appendix Figure S5

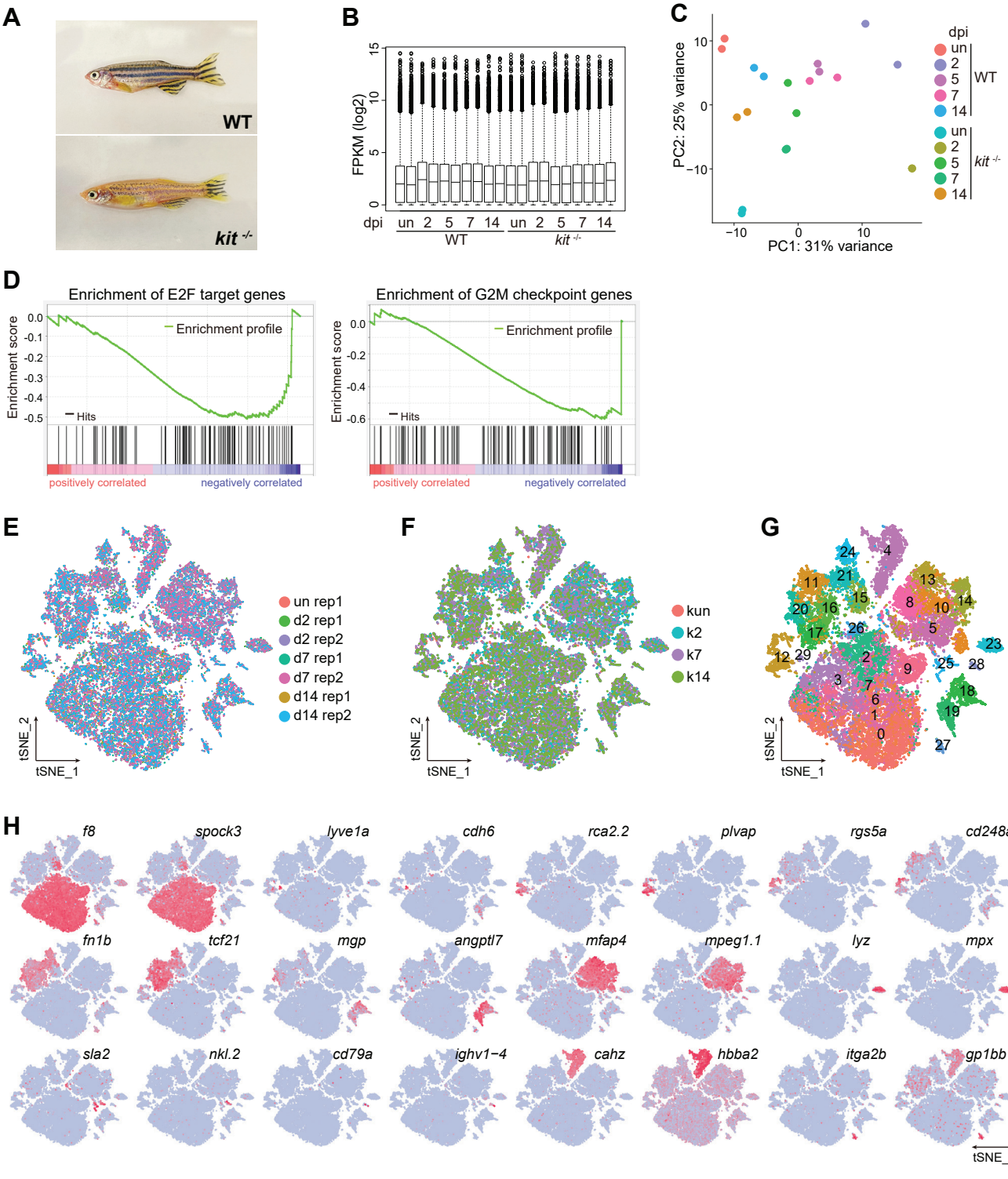

Appendix Figure S6

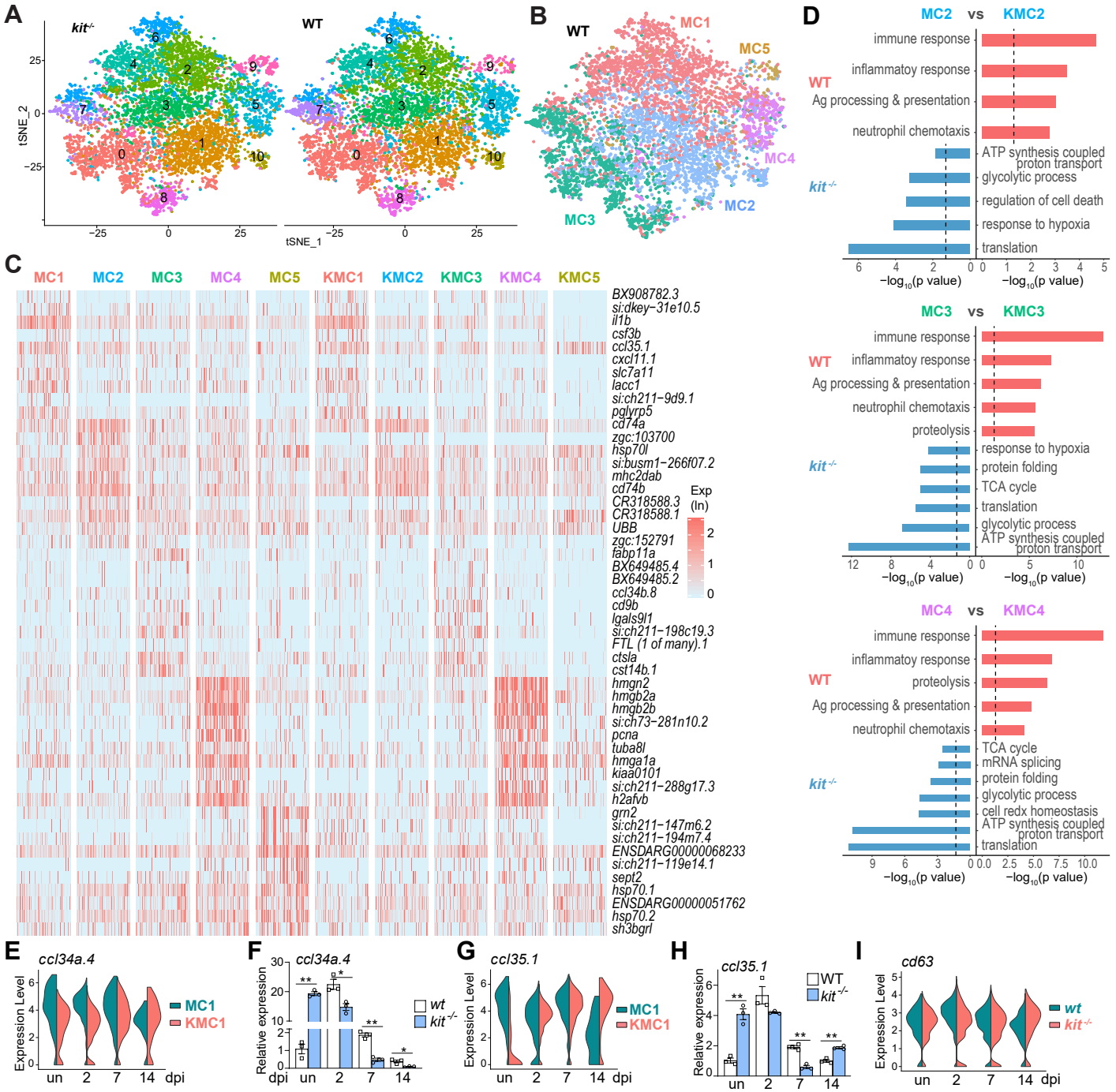

Appendix Figure S7

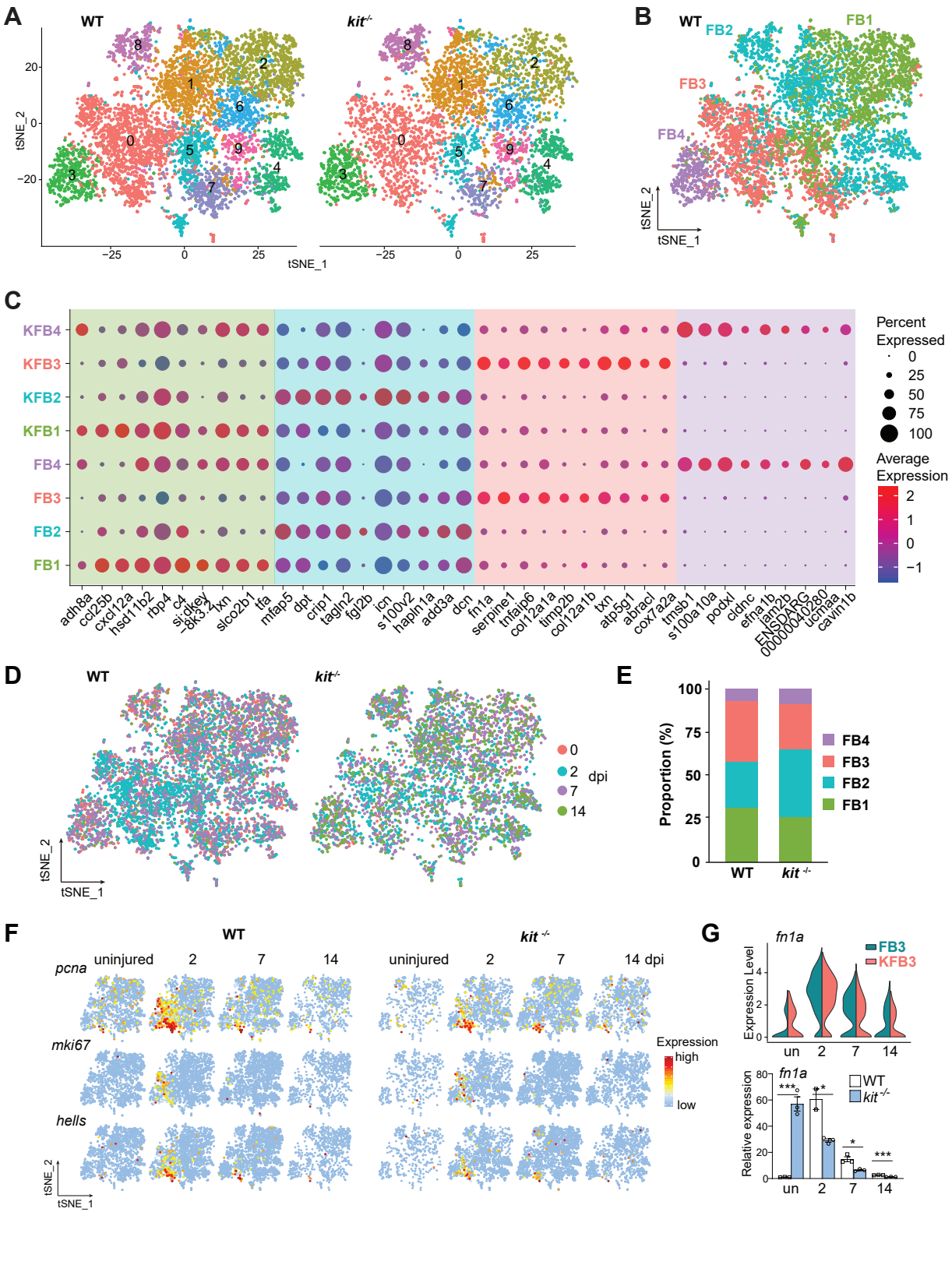

Appendix Figure S8

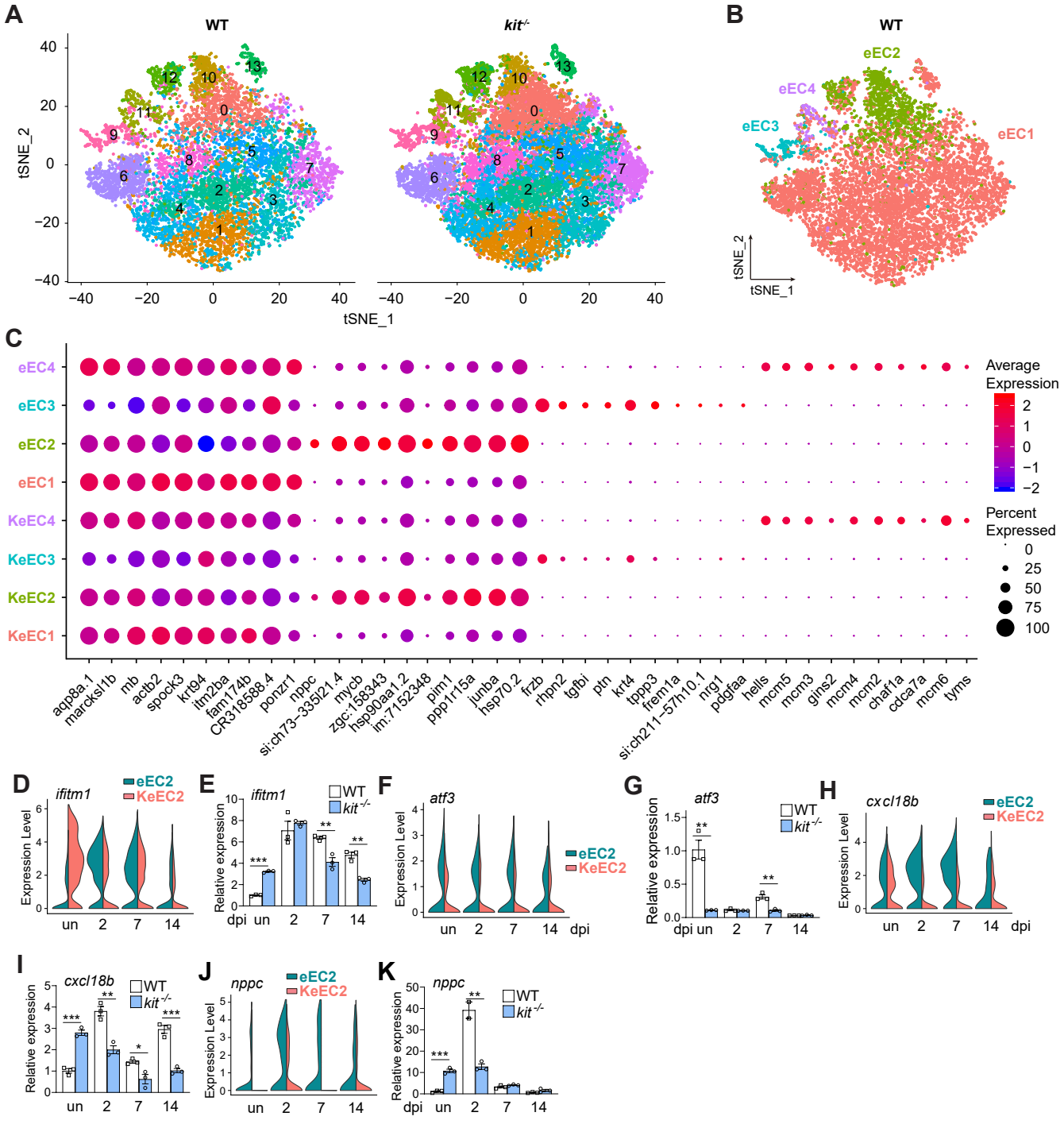

Appendix Figure S9

Appendix Table S1

sample	ncells	median_nGene	median_nUMI	median_mito_percent
wt_d0_a	2381	696	2710	15.35%
wt_d0_b	4660	662	2640.5	17.54%
wt_d2_a	836	1431	6606	0.59%
wt_d2_b	8866	884	3448.5	6.88%
wt_d7_a	1628	775.5	2926.5	2.07%
wt_d7_b	5647	720	3162	11.42%
wt_d14_a	3147	864	3783	7.59%
kit$^{-/-}$_d0_a	4203	918	3756	6.18%
kit$^{-/-}$_d2_a	1629	1121	4987	2.56%
kit$^{-/-}$_d2_b	9355	615	2114	20.95%
kit$^{-/-}$_d7_a	6380	655	2684.5	16.05%
kit$^{-/-}$_d7_b	7080	794	3521	12.54%
kit$^{-/-}$_d14_a	2085	1144	5055	3.39%
kit$^{-/-}$_d14_b	4080	766.5	3163	14.76%

Appendix Table S2

Name	Sequence (5' - 3')
il1b-RT-F	CGCTCCACATCTCGTACTCA
il1b-RT-R	ATACGCGGTGCTGATAAACC
ccl35.1-RT-F	GTTATGGTGCTGCTGTGTGC
ccl35.1-RT-R	GTCTTGAACAGGACGGCTTC
ctsd-RT-F	TCGCTAAGGCCAAATCAGTC
ctsd-RT-R	CGGTTTGACTTTTCCCTGAA
col12a1a-RT-F	ATGCCTTACAACGGACAAGG
col12a1a-RT-R	GGAGGCTTGCAGTTTTTGAC
fn1a-RT-F	ATGCTTTCGACCGATACAGG
fn1a-RT-R	CTGGGCGTGATTTTACAGGT
mif-RT-F	AATGTGGCCTGGAACAACAG
mif-RT-R	CAAGATGCTGTCTGCCGTAA
ifitm1-RT-F	AGCCACCAATAACCCTTCAA
ifitm1-RT-R	TTGCTGAGATCACACCATGAG
junba-RT-F	ACGGACTCTGGGAAACACTG
junba-RT-R	ATGTTTTCAAAGGGCAGCAC
nppc-RT-F	CGTCCCACTACCACTCCATT
nppc-RT-R	AGCTTTCCTCATCCTCGTCA
cxcl18b-RT-F	CAGCTCTGCTTGAATCCACA
cxcl18b-RT-R	CTTGCTCAGACTCCCTGGAC
elfa-RT-F	CTTCTCAGGCTGACTGTGC
elfa-RT-R	CCGCTAGCATTACCCTCC
fn1-ISH-F	TGATTGGAAAGGCAAGAACTC
fn1-ISH-R	CCCTCGTCATAACAGGTGG
fn1b-ISH-F	CAATAATCAGCCCAAACAACC
fn1b-ISH-R	TCGTGACACCATTTGGAAGAG
gstm.3-ISH-F	TTGCTCAACCAGTCCGTCTAC
gstm.3-ISH-R	TGGCCATCTTGTTGTTCACAG

Appendix Table S3

Sample	num pairs	matched pairs
wt_d0-1	35794165	94.46%
wt_d0-2	40701810	93.26%
wt_d2-1	32156273	92.87%
wt_d2-2	21670210	93.23%
wt_d5-1	37821605	93.63%
wt_d5-2	38810223	93.85%
wt_d7-1	41880606	93.79%
wt_d7-2	30300968	96.28%
wt_d14-1	27247944	93.48%
wt_d14-2	38296161	94.45%
kit_d0-1	41201729	96.19%
kit_d0-2	36091498	95.44%
kit_d2-3	61801678	93.78%
kit_d2-4	59063891	94.48%
kit_d5-1	37022079	96.50%
kit_d5-2	43813868	96.59%
kit_d7-1	41472840	95.84%
kit_d7-2	37885800	95.63%
kit_d14-1	40197195	95.49%
kit_d14-2	39345770	96.30%

Appendix Figure Legends

Appendix Figure S1. Single-cell transcriptomics reveals heterogeneity of zebrafish cardiac nonCMs. Related to Fig. 1.

A-B, nonCMs visualized on tSNE and colored by LIGER clusters (A) or experiment replicates (B). **C**, tSNE plots showing expression of additional canonical markers of nonCM populations: *flt1* (EC), *mpeg1.1* (MC), *lck* (T cells), *nkl.2, zbtb32* (NK cells), *cd79a* (B cells), *cahz, slc4a1a* (erythrocyte), *itga2b* and *gp1bb* (thrombocyte). Related to Fig. 1B-D. **D-F**: Zoom-in analysis of nonCMs expressing canonical EC markers (EC in Fig. 1B-C). Related to Fig. 1E-G. **D-E**, Cells visualized on tSNE and colored by experiment replicates (D) or LIGER clusters (E). **F**, tSNE plots showing expression of reported EC markers used to assign EC subtypes: *kdrl* and *cdh5* (pan-EC markers), *lyve1a* and *prox1a* (lymphatic EC), *rgs5a, cd248a, acta2,* and *tagln* (mural cells), *gata5* (endocardial EC), and others for coronary ECs. **G**, tSNE plots showing differential expression pattern of different arterial markers and cadherins in EC subpopulations: pan-cardiac EC *notch1b* and coronary-specific *hey1* and *pcdh18a*. **H**, Heatmap of inter-cell type Pearson correlation coefficient of pseudo-bulk transcriptome of EC and mural cells. **I**. More GO terms and p values for Fig. 1C.

Appendix Figure S2. Transcriptome dynamics of cardiac nonCM during heart regeneration. Related to Fig. 2. Joint analysis of nonCM scRNA-seq data from uninjured hearts and hearts at 2, 7, and 14 dpi with LIGER. **A**, tSNE plot showing the integration of all datasets using CCA algorithm in Seurat v2.3.4. Cells clustered by time points rather than cell type. **B-C**, tSNE plot showing the integration of all datasets using LIGER. Cells colored by time points (B) or experiment replicates (C). **D**, tSNE plots colored by percentage of mitochondrial UMI (top) or

number of genes detected (bottom). Clustering of each cell type was not affected by mito % or nGene. **E-F**, NonCMs visualized on tSNE and colored by in silico assigned cell cycle phase (E) or LIGER clusters (F). Clustering of each cell type was not affected by cell cycle stages. **G**, tSNE plots showing expression of cell type markers identified in Fig. 1 that were used to assign cell type to each LIGER cluster in (F). **H**, Heatmap showing expression of top 10 markers of each nonCM cell type. The bar below each cell type demonstrates the relative proportion of cells from corresponding time point, suggesting that these cell types were detected at all time points.

Appendix Figure S3. Zoom-in analysis of macrophage transcriptome dynamics revealed five distinct MC subpopulations during heart regeneration. Related to Fig. 2.

A, Macrophages identified in Fig.2 were zoom-in analyzed with LIGER and cells were visualized on a tSNE plot colored by LIGER-assigned clusters. **B,** Heatmap of inter-cluster Pearson correlation coefficient of pseudo-bulk transcriptome of clusters in A. **C,** Expression levels of canonical macrophage markers, *mfap4* and *mpeg1.1*, color-coded and mapped onto the tSNE embeddings in A. **D-E,** Positive markers for each MC subpopulation was calculated with the FindAllMarkers function in Seurat and GO analysis was performed with these lists of positive markers in DAVID/6.8. **D**, Heatmap showing expression of top 10 positive markers (ranked by fold change) of each MC subpopulation. Genes mentioned in the results section was highlighted in red. **E**, Representative GO terms and p values and violin plots of additional representative markers for each MC subpopulation. **F**, MC visualized on tSNE and colored by time points. **G,** Expression levels of pro-inflammatory cytokines *ccl35.1*, *ccl34.4*, and *cxcl11.1* in MC at indicated time points color-coded and mapped onto tSNE. **H**, Violin plots showing expression of *cd74a* and *mhc2dab* (MC2 markers) in MC2 at different time points along regeneration. **I,** Violin plots

showing expression of *cd63, ctsd* and *ctsla* in MC subpopulations. **J**, *In silico* assigned cell cycle phase of each MC cell color-coded and mapped onto tSNE. **K-L,** Expression levels of *grn1* (K) and *tgfb1a* (L) in MC at indicated time points color-coded and mapped onto tSNE.

Appendix Figure S4. Zoom-in analysis of fibroblast transcriptome dynamics identified an activated FB subpopulation transiently expanded post injury during heart regeneration. Related to Fig. 3.

A, Fibroblasts identified in Fig.2 were zoom-in analyzed with LIGER and cells were visualized on a tSNE plot colored by LIGER-assigned clusters. **B,** Heatmap of inter-cluster Pearson correlation coefficient of pseudo-bulk transcriptome of clusters in A. **C,** Expression levels of canonical fibroblast markers, *tcf21, fn1b* and *col1a1a*, color-coded and mapped onto the tSNE embeddings in A. **D**, Positive markers for each FB subpopulation was calculated with the FindAllMarkers function in Seurat and GO analysis was performed with these lists of positive markers in DAVID/6.8. Top, Dotplot showing expression of top 10 positive markers (ranked by fold change) of each FB subpopulation. Genes mentioned in the results section was highlighted in red. Bottom, Representative GO terms and p values for each FB subpopulation. **E**, Expression levels of ECM genes *fn1b, dcn* and *sparc* in FB at indicated time points color-coded and mapped onto tSNE. **F**, FB visualized on tSNE and colored by time points. **G**, *In silico* assigned cell cycle phase of each FB cell color-coded and mapped onto tSNE. **H-I**, Expression levels of canonical cell cycle genes *pcna, mki67*, and *hells* (H), and ECM genes *col12a1b* and *postnb* (I) in FB at indicated time points color-coded and mapped onto tSNE. **J**, Violin plots showing the expression of *gstm.3* in FB3 at different time points. **K,** *In situ* hybridization showing temporal spatial expression patterns of *fn1b*. Blue dashed lines indicate approximate resection plane. Scale bar: 50 μm. **L**, Temporal and spatial patterns of *tnfa:GFP* positive MC1 cells. White dashed lines indicate approximate resection plane. **M**, Heatmap showing number of upregulated and downregulated genes in each FB subpopulation post injury. Differential expressed genes (DEG) calculated with the

FindMarkers function in Seurat (logfc.threhold = 0.15). Numbers of DEG for each comparison were labeled on the heatmap. **N**, Expression levels of transcription regulators *fosl2, sap18, phb2b* and *prmt1* in FB at indicated timepoints color-coded and mapped onto tSNE.

Appendix Figure S5. Zoom-in analysis of endocardial EC transcriptome dynamics revealed interesting interplay between MC and EC during heart regeneration. Related to Fig. 3.

A, eEC identified in Fig.2 were zoom-in analyzed with LIGER and cells were visualized on a tSNE plot colored by LIGER-assigned clusters. **B,** Heatmap of inter-cluster Pearson correlation coefficient of pseudo-bulk transcriptome of clusters in a. **C,** Positive markers for each eEC subpopulation was calculated with the FindAllMarkers function in Seurat and GO analysis was performed with these lists of positive markers in DAVID/6.8. Top, Dotplot showing expression of top 10 positive markers (ranked by fold change) of each eEC subpopulation. Genes mentioned in the results section was highlighted in red. Bottom, Representative GO terms and p values for each eEC subpopulation. **D**, Expression of *nppc* in each eEC subpopulation shown as violin plots (left) or split by time points, color-coded and mapped onto the tSNE embeddings in a (right). **E**, Violin plots showing the expression of *cxcl18b, sele, atf3* and *fosl1a* in eEC at different time points. **F**, Violin plots showing expression of eEC3 markers *frzb, bmp6, tgfbi* and *wnt11r* in each eEC subpopulation. **G**, *In silico* assigned cell cycle phase of each eEC cell color-coded and mapped onto tSNE. **H**, Expression levels of canonical cell cycle genes *pcna, hells* and *mcm3* shown as violin plots (left), or split by time points, color-coded and mapped onto tSNE.

Appendix Figure S6. Loss of *kit* function impairs heart regeneration. Related to Fig. 4.

A, Adult wildtype (WT) and *kit* mutant zebrafish. Note that the wildtype zebrafish has melanocyte stripes in the body. **B-D**, Analysis of bulk RNA-seq data of freshly isolated CMs at 5 different time points during heart regeneration. **B**, Boxplot showing distribution of gene expression of indicated samples. Median expression was shown as a line in the box and outliers were shown as dots. **C**, PCA plot using all genes showed the consistency of biological replicates in each condition. **D**, Two representative gene sets from GSEA analysis, which are enriched in DEGs between *kit* mutant and wildtype CM at 7 dpi. **E-H**, Joint analysis of *kit* mutant nonCM scRNA-seq data from uninjured hearts and hearts at 2, 7, and 14 dpi with LIGER. **E-G**, tSNE plots showing the integration of all datasets using LIGER. Cells colored by experiment replicates (E), time points (F) or LIGER clusters (G). **H**, tSNE plots showing expression of cell type markers identified in Fig. 1 that were used to assign cell type to each LIGER cluster in (G).

Appendix Figure S7. Joint analysis of WT and *kit* mutant macrophages during heart regeneration. Related to Fig. 5.

A, Macrophages identified in Fig.2 (WT) and Fig. 3 (*kit* mutant) were jointly analyzed with LIGER and cells were visualized on side-by-side tSNE plots split by genotypes and colored by LIGER-assigned clusters. **B,** WT MC cells projected onto the tSNE embedding from joint analysis in (a) and colored by subtype assignment in Fig. 2C. **C,** Heatmap showing expression of top 10 positive markers of each WT MC subpopulation (Extended Data Fig. 3D) in each WT and *kit* mutant MC subpopulations assigned in Fig. 4A. **D**, Representative GO terms of genes upregulated in WT MC subpopulations (orange bars) or their corresponding *kit* mutant MC populations (blue bars) from the uninjured heart when compared to each other. **E, G**, **I,** Violin plots showing expression of

ccl34a.4 (E) and *ccl35.1* (G) in WT and *kit* mutant MC1, and expression of *cd63* in MC (I). **F**, **H**, Expression of *ccl34a.4* (F) and *ccl35.1* (H) in WT and *kit* mutant hearts determined by qRT-PCR. Data are presented as Mean ± SEM. N = 3. P value calculated with two-tailed students' t test. * P < 0.05, ** P < 0.01.

Appendix Figure S8. Joint analysis of WT **and *kit* mutant fibroblasts during heart regeneration.** Related to Fig. 5.

A, Fibroblasts identified in Fig.2 (WT) and Fig. 3 (*kit* mutant) were jointly analyzed with LIGER and cells were visualized on side-by-side tSNE plots split by genotypes and colored by LIGER-assigned clusters. **B,** WT FB cells projected onto the tSNE embedding from joint analysis in (A) and colored by subtype assignment in Fig. 2G. **C,** Dot plot showing expression of top 10 positive markers of each WT FB subpopulation in each WT and *kit* mutant FB subpopulations assigned in Fig. 4H. **D**, WT and *kit* mutant FB visualized on tSNE and colored by time points. **E,** Bar plots showing proportion of each WT and *kit* mutant FB subpopulation in FB. **F**, Expression levels of canonical cell cycle genes *pcna, mki67*, and *hells* in WT and *kit* mutant FB at indicated time points color-coded and mapped onto tSNE. **G**, Violin plots and qRT-PCR showing expression of *fn1a* in FB3. Data are presented as Mean ± SEM. N = 3. P value calculated with two-tailed students' t test. * P<0.05, *** P<0.01.

Appendix Figure S9. Joint analysis of WT **and *kit* mutant endocardial EC during heart regeneration.** Related to Fig. 5.

A, Endocardial EC identified in Fig. 2 (WT) and Fig. 3 (*kit* mutant) were jointly analyzed with LIGER and cells were visualized on side-by-side tSNE plots split by genotypes and colored by LIGER-assigned clusters. **B,** WT eEC cells projected onto the tSNE embedding from joint analysis

in (A) and colored by subtype assignment in Fig. 2N. **C,** Dot plot showing expression of top 10 positive markers of each WT eEC subpopulation (Fig. S5C) in each WT and *kit* mutant eEC subpopulations assigned in Fig. 4O. **D, F, H, J,** Violin plots showing expression of *ifitm1* in eEC; *atf3*, *nppc* and *cxcl18b* in eEC2**. E, G, I, K** Expression of *ifitm1*, *atf3*, *nppc* and *cxcl18b* in WT and *kit* mutant hearts determined by qRT-PCR. Mean ± SEM shown. N = 3. P value calculated with two-tailed students' t test. ** $P < 0.01$.

Appendix Table Legends

Appendix Table S1. Summary of post-QC sequencing metrics of each scRNA-seq sample.

Appendix Table S2. Sequences of primers used for in situ hybridization and qRT-PCR.

Appendix Table S3. Mapping summary of bulk RNA-seq samples.